Photosynth Res
DOI 10.1007/s11120-013-9839-9

REGULAR PAPER

Kinetics and functional diversity among the five members of the NADP-malic enzyme family from *Zea mays*, a C_4 species

Clarisa E. Alvarez · Mariana Saigo · Ezequiel Margarit · Carlos S. Andreo · María F. Drincovich

Received: 22 February 2013 / Accepted: 25 April 2013

Abstract NADP-malic enzyme (NADP-ME) is involved in different metabolic pathways in several organisms due to the relevant physiological functions of the substrates and products of its reaction. In plants, it is one of the most important proteins that were recruited to fulfil key roles in C_4 photosynthesis. Recent advances in genomics allowed the characterization of the complete set of NADP-ME genes from some C_3 species, as *Arabidopsis thaliana* and *Oryza sativa*; however, the characterization of the complete NADP-ME family from a C_4 species has not been performed yet. In this study, while taking advantage of the complete *Zea mays* genome sequence recently released, the characterization of the whole NADP-ME family is presented. The maize NADP-ME family is composed of five genes, two encoding plastidic NADP-MEs (ZmC_4- and Zm*non*C_4-NADP-ME), and three cytosolic enzymes (Zmcyt1-, Zmcyt2-, and Zmcyt3-NADP-ME). The results presented clearly show that each maize NADP-ME displays particular organ distribution, response to stress stimuli, and differential biochemical properties. Phylogenetic footprinting studies performed with the NADP-MEs from several grasses, indicate that four members of the maize NADP-ME family share conserved transcription factor binding motifs with their orthologs, indicating conserved physiological functions for these genes in monocots. Based on the results obtained in this study, and considering the biochemical plasticity shown by the NADP-ME, it is discussed the relevance of the presence of a multigene family, in which each member encodes an isoform with particular biochemical properties, in the evolution of the C_4 NADP-ME, improved to fulfil the requirements for an efficient C_4 mechanism.

Keywords Maize · NADP-malic enzyme · C_4 photosynthesis · Orthologs · Evolution

Introduction

NADP-malic enzyme (NADP-ME; L-malate: NADP oxidoreductase [OAA decarboxylating], EC 1.1.1.40) catalyses the reversible oxidative decarboxylation of L-malate to yield pyruvate, CO_2 and NADPH. Considering the relevant physiological functions of both the substrates and products of the NADP-ME reaction, this enzyme is widely distributed among eukaryotes and prokaryotes, where is involved in different metabolic pathways. Several studies have related NADP-ME with plant functions as diverse as lipid biosynthesis (Smith et al. 1992; Eastmond et al. 1997), defence responses (Casati et al. 1999; Schaaf et al. 1995), control of cytosolic pH (Martinoia and Rentsch 1994), and stomata opening (Outlaw et al. 1981; Laporte et al. 2002), among others. Nevertheless, one of the most outstanding roles of NADP-ME is to provide CO_2 to RuBisCO in the

Clarisa E. Alvarez and Mariana Saigo contributed equally to this study.

Electronic supplementary material The online version of this article (doi:10.1007/s11120-013-9839-9) contains supplementary material, which is available to authorized users.

C. E. Alvarez · M. Saigo · E. Margarit · C. S. Andreo · M. F. Drincovich (✉)
Centro de Estudios Fotosintéticos y Bioquímicos (CEFOBI), Universidad Nacional de Rosario, Suipacha 531, Rosario, Argentina
e-mail: drincovich@cefobi-conicet.gov.ar

Present Address:
E. Margarit
Instituto de Biología Molecular Rosario (IBR) Esmeralda y Ocampo, Edificio IBR-Predio CCT, Rosario, Argentina

Published online: 07 May 2013

chloroplasts of the bundle sheath cells (BSC) of some C_4 plants (Drincovich et al. 2010), allowing a highly efficient photosynthetic process due to the raise of CO_2/O_2 ratio at the site of RuBisCO (Hatch 1987). Thus, C_4 plants have a better performance under diverse environmental conditions such as high light intensities, high temperatures, or poor water availability (Edwards and Walker 1983). In the last decades, with the aim of the introduction of C_4 traits in C_3 plants, more sophisticated approaches have been extensively explored toward the understanding of how C_4 photosynthesis evolved and how it is regulated (Langdale 2011). These studies have indicated that proteins recruited into C_4 photosynthesis are already present in C_3 species fulfilling nonphotosynthetic roles (Aubry et al. 2011). In the case of NADP-ME, recent advances in genomics have allowed the characterization of the complete set of NADP-ME genes from some C_3 species, as *Arabidopsis thaliana* (Gerrard Wheeler et al. 2005) and rice (*Oryza sativa*, Chi et al. 2004). The NADP-ME family of these C_3 model species, dicot, and monocot, respectively, is composed of three cytosolic and one plastidic NADP-ME members. However, the characterization of the complete NADP-ME family from a C_4 species, has not been performed yet.

Maize (*Zea mays*) is a highly productive monocot species that has been extensively used as paradigm for C_4 studies (Li et al. 2010; Pick et al. 2011). At present, three NADP-ME isoforms have been characterized in maize: one plastidic involved in C_4 photosynthesis (C_4-NADP-ME, Detarsio et al. 2003; 2007), a second plastidic nonphotosynthetic isoform that responds to plant defence inducers (*non*C_4-NADP-ME, Saigo et al. 2004; 2013), and one cytosolic isoform abundant in embryo tissues (cyt-NADP-ME, López-Becerra et al. 1998; Detarsio et al. 2008). Nevertheless, the recently released genomic maize sequence (Schnable et al. 2009) reveals the existence of two other genes encoding putative NADP-ME isoforms, which properties and expression in this C_4 model species have not been studied yet. In this study, we present the first characterization of the whole NADP-ME family of a C_4 grass. The comparison of the NADP-ME multigene family from different grasses allowed the identification of conserved expression regulation of some orthologs. Furthermore, the level of expression of each NADP-ME in different maize organs and under different conditions combined with *in silico* prediction of regulatory sites and kinetic studies of the uncharacterized isoforms indicate that albeit very similar in amino acid sequence and in some cases subcellular colocalization, each isoform would have distinctive roles in maize life. Finally, the importance of a multigene NADP-ME family as a starting point in the evolution of NADP-ME isoforms with distinct physiological roles is discussed.

Methods

Plant material

Maize (*Zea mays*) plants (hybrid AX882 Nidera) were cultivated in greenhouse conditions under a 12-h light/12-h dark regime at a photosynthetically active photon flux density (PPFD) of 300 μmol quanta m^{-2} s^{-1}. For the expression profile analysis, seven different samples were selected: leaf blades (L); stems (St); and roots (R), of 15 days old seedlings; leaf sheaths (Sh); immature ears (1–2 cm, E); and immature tassels (1.5–2 cm, T) of mature plants (6–8 weeks old) and developing grains (G) collected at 7, 14, 20, and 27 days after pollination (DAP). For a more detailed analysis of the distribution of NADP-MEs transcripts in the leaf, 4 cm segments from the base, middle and tip of a 40-cm long leaf blade were sampled. Stress treatments were evaluated in 15-day-old maize seedlings. The treatments were performed by dipping the roots in solutions containing: 60 mM $NaHCO_3$ pH 8.0; 30 mM Na_2CO_3 pH 11.0; or 0.5 % (w/v) cellulase for 6 h. Treatment with 250 μM of abscisic acid (ABA) was performed in the same way but for 3 h. Control plants for these treatments were incubated in water for the same time of each treatment. UV treatment was performed by exposing the seedlings for 4 h with an intensity of 2 W m^{-2}. Leaves, roots, and stems were collected at the end of each treatment. Pools of three different plants were made for each biological repetition. In all cases, the samples collected were immediately frozen in liquid N_2 and stored at −70 °C until processing.

RNA extraction and reverse transcription reaction

Total RNA was isolated from 100 mg of each tissue of maize using the Trizol reagent (Gibco-BRL) following the recommendations of the manufacturer. The concentration and integrity of the preparations were assayed by agarose 2 % gel electrophoresis. Two micrograms of total RNA were reverse transcribed with 200 U of M-MLV reverse transcriptase (Promega) using oligodT as primer. The cDNAs were used as templates for quantitative PCR assays or clonning.

Quantitative real-time PCR analysis

Relative gene expression was determined by quantitative real-time PCR (qRT-PCR) on a Mx3000P detection system and the MxPro–Mx3005P software version 4.01 (Stratagene). Primers were designed using Primer Select of DNAStar Lasergene version 10.1 (DNASTAR, Madison, WI, USA) to allow for amplification of 150–250 bp products of similar GC and Tm characteristics. The generation

of specific PCR products was confirmed by melting curve, gel analysis, and PCR amplification using plasmids containing the cDNAs of each isoform, respectively. The PCR mix contained SYBR® Green I 1× (Invitrogen); 2.5 mM $MgCl_2$; 0.5 µM of each primer; 0.05 U/µl Platinum Taq; and 1× buffer provided by the manufacturer (Invitrogen). Tenfold dilutions of the cDNAs synthesized as described above from different maize tissues were used as templates. Thermal cycling parameters were as follows: initial denaturation at : 94 °C for 2 min for initial denaturation; 45 cycles of 96 °C for 10 s; and 58 °C for 15 s; 72 °C for 35 s for amplification products by PCR and 10 min at 72 °C for final elongation. Denaturation curves for each PCR reaction were determined by measuring the decrease in fluorescence with increasing temperature from 65 to 98 °C.The *actin1* gene was used as reference (Veach et al. 2003; Manoli et al. 2012). Relative gene expression was calculated using a modified version of the comparative $2^{-\Delta\Delta}C_T$ method (Pfaffl 2001), the efficiencies were calculated as described by Liu and Saint (2002), and the error propagation according to Hellemans et al. (2007). The oligonucleotide primers pairs used are: ZmC_4-NADP-ME: C_4left 5′-ACAGTTCTGATCGGGACATC-3′ and C_4right 5′-CG AGTCCAGGGAAAATGT AG-3′; Zm*non*C4-NADP-ME: nonC_4left 5′-AGATTTCAAAACAGACGTCG-3′ and nonC_4-right 5′-GGAAGCCATGGCCTCAACAAC-3′; Zmcyt1-NADP-ME: Cyt1right 5′-CTATTCCGCAGCGTTTATC TCTT-3′ and Cyt1left 5′-AAGGACGGCAC CAGCACC AT-3′; Zmcyt2-NADP-ME: Cyt2left 5′-AGAGCCATCTCG TCTTCAAC-3′ and Cyt2right 5′-AGTCCATCAGCCAGA TCTTC-3′; Zmcyt3-NADP-ME: Cyt3left 5′-TCTAGGGGT GGTGATCT-3′ and Cyt3right 5′-AGTCCATCAGCCAG ATCTTC-3′ actF: 5′-GAGGCCACGTACAACTCCA-3′ and actR: 5′-AATAGAGCCAGGGATCCAGA-3′. The absence of mispriming among NADP-MEs primers was confirmed by the absence of amplification when crossing primers and targets (NADP-MEs cDNAs) in PCR assays.

Cloning of Zmcyt1-NADP-ME and Zmcyt2-NADP-ME cDNAs

Zea mays cDNAs encoding Zmcyt1-NADP-ME and Zmcyt2-NADP-ME were amplified by RT-PCR using RNA extracted from leaves with the TRIZOL reagent (Gibco-BRL). Amplification was conducted using M-MLV (Promega) and specific primers. In the case of Zmcyt1-NADP-ME, the oligonucleotide pair: Cyt1-up 5′-A**GA TAT**CGCTTCGGGTTCGGCGAAGG-3′ and Cyt1-down 5′-A**CTCGAG**TC AACGGTAGTTGCGGTAGATG-3′ was used. Zmcyt2-NADP-ME was amplified with the primer pair: Cyt2-up 5′-**GGATCC**ATGGCGGGCGGCGGC GTTGCG-3′ and Cyt2-down 5′-**AAGCTT**TTACCGGTA GCTGCGGTAGATGG-3′. The oligonucleotides were designed to introduce particular restriction sites used to clone in pET32 expression vector (underlined). Then, the PCR products were cloned into pGEMT-easy vectors (Promega) and completely sequenced. The corresponding cDNAs were subcloned into pET32a vector downstream of an inducible T7 promoter system (Novagen).

Heterologous expression of Zmcyt1- and Zmcyt2-NADP-ME

In each pET32a vector containing the inserts of Zmcyt1- and Zmcyt2-NADP-ME, the NADP-ME is fused in frame to the His-tag to facilitate purification of the expressed fusion protein by a nickel-containing His-bind column (Novagen). The induction and purification of the fusion proteins were performed as previously described for other maize MEs with minor modifications (Detarsio et al. 2003; Saigo et al. 2004). The fusion proteins were then concentrated on Microcon 30 K (Millipore) using buffer TMG (50 mM Tris–HCl pH 8.0; 10 mM $MgCl_2$, and 10 % (v/v) glycerol). Then, purified fusion NADP-ME proteins, Zmcyt1- and Zmcyt2- were incubated with enterokinase 1:5 and 1:10 w/w in buffer TMG at 16 °C for 2 h, respectively, to remove the N-terminus encoded by the expression vector. The purity and integrity of the proteins obtained were examined by SDS-PAGE, and the concentration was estimated using the Bradford method and the absorbance at 280 nm. The purified enzymes were immediately stored in small aliquots at −70 °C in buffer TMG.

NADP-ME activity assays

NADP-malic enzyme activity was determined spectrophotometrically using a standard reaction mixture containing 50 mM Tris–HCl pH 8.0; 10 mM $MgCl_2$; 0.5 mM NADP; and 10 mM L-malate. Initial velocity studies were performed by varying the concentration of one of the substrates around its K_m value while keeping the other substrate at saturating levels. All kinetic parameters were calculated at least by triplicate determinations and adjusted to nonlinear regression using concentrations of all substrates (Detarsio et al. 2003). One unit is defined as the amount of enzyme that catalyses the formation of 1 µmol of NADPH min^{-1} under the specified conditions.

Phylogenetic analyses

The phylogenetic tree was inferred by neighbor joining method (NJ) using MEGA 5.10 software (Tamura et al. 2011). In order to evaluate the robustness of the tree structure, 500 replicates of bootstrap searches were performed using maximum parsimony (MP) and neighbor joining (NJ) in MEGA 5.10. Besides the five *Zea mays* isoforms of NADP-ME described in this article (ZmC_4-, Zm*non*C_4-,

Zmcyt1-, Zmcyt2-, and Zmcyt3-NADP-ME), the following sequences were evaluated: C3(1) and C3(2) of *A. thaliana* (ME 1–4 Gerrard Wheeler et al. 2005; Q9XGZ0; Q9LYG3; O82191; Q9CA83, respectively); C4(2) of *Flaveria trinervia* (ME1 and ME2, CAA40421 Borsch and Westhoff 1990; and ABS32243 Saavedra et al. unpublished, respectively); C4(2) of *Flaveria palmeri* (ABSS32241); C4(2) from *Flaveria bidentis* (AAW56450); CAM(1) of *Mesembryanthemun crystallinum* (P37223, Cushman 1992); CAM(1) of *Aloe arborescens* (BAA74735, Honda et al. 2000); CAM(2) of *Aloe arborescens* (BAA24950, Honda et al. 1997); C3(1) of *Phaseolus vulgaris* (P12628, Walter et al. 1994); *Populus trichocarpa* (P34105, Van Doorsselaere et al. 1991); C3(1) and C3(2) of *Vitis vinifera* (P51615, Franke and Adams 1995, and AAB08874); C3(1) *Solarum lycopersicum* (*1 and 2*, nP_001234458, and NP_001233951, respectively), and C3(2) of *S. lycopersicum1* (P37222); *Apium graveolens* (CAB66003); *Nicotiana tabacum* (ABI98681, Müller et al. 2008); CAM(1) *Hydrilla verticalla* (*1 to 3*, AAT02533; AAT02534; AAT02535, respectively, Estavillo et al. 2007); C3(1) of rice (*O. sativa*; OscytME 1, 2 and 3, BAB20887; NP_001054832; EAZ13499; respectively; Chi et al. 2004); C3(2) of rice (OschlME BAA0349 *O. sativa*; Fushimi et al. 1994); C3(1) of *Flaveria pringlei* (*A and B*, AAK83073, and AAK83074, respectively, Lai et al. 2002); and C3(2) of *Flaveria pringlei* (P36444, Lipka et al. 1994); C4(1) of *Setaria italica* (*1 to 3*, Si000645m; Si000774m; Si000808m; respectively) and C4(2) of *Setaria italica* (Sichl, C8ZK26); *Prunus persica* (AFR54473) and *Prunus persica1 to 3* (PPA002714m; PPA003214m; PPA003210m; respectively); C4(1) of *Sorghum bicolor* (*1 to 3*, Sb09g005810.1; Sb03g034280.1; Sb03g033250; respectively) and C4(2) of *S. bicolor* (*1 to 3*, Sb03g003230; Sb09g017550; Sb03g003220; respectively); C3(1) of *R. communis1 and 2* (XP_002516526 and XP_002514230, respectively). The nomenclature used for each enzyme includes the photosynthetic type (CAM, C_3, or C_4) followed by a number, which indicates the subcellular localization of each enzyme (1 for cytosolic and 2 for plastidic; Drincovich et al. 2001).

Identification of transcription factor binding sites

In silico mapping of conserved transcription factor binding sites in NADP-ME genes was carried out using multiple-sequence local alignment (MULAN) for sequences alignment and MultiTF for transcription factor binding motifs search in TRANSFAC database (Ovcharenko et al. 2005). NADP-ME gene sequences from sorghum (*Sorghum bicolor*), *Setaria italica* and rice (*O. sativa*) were retrieved from Phytozome (http://www.phytozome.net/, Goodstein et al. 2011). The orthologs of each maize NADP-ME gene were identified by sequence similarity (ClustalW, Fig. 2) and syntheny, according to the information available at Phytozome. In brief, orthologous NADP-ME gene sequences along with their 1,000 bp upstream and downstream regions were aligned with MULAN and combined with a transcription factor binding site (TFBS) search using Transfac Professional positional weight matrixes. Then, MultiTF scanned through each of the predictions searching for TFBS present among all genes and in conserved regions previously aligned. The search of transcription factors coexpressed with rice NADP-ME genes was performed using RiceFREND (http://ricefrend.dna.affrc.go.jp/; Sato et al. 2013).

Results

The NADP-malic enzyme gene family from maize is composed of five members

The complete sequence of the maize genome allowed us to find out all the members of the NADP-ME family, which resulted composed of two plastidic enzymes: ZmC_4-NADP-ME (*nadpme-IVc* gene, GRMZM2G085019, Detarsio et al. 2003) and Zm*non*C_4-NADP-ME (*nadpme-IVa* gene, GRMZM2G122479, Saigo et al. 2004); a cytosolic isoform: Zmcyt3-NADP-ME (*nadpme-I* gene, GRMZM2G118770, previously named as Zmcyt-NADP-ME in Detarsio et al. 2008); and two putative cytosolic isoforms: Zmcyt1- (*nadpme-II* gene, GRMZM2G085019) and Zmcyt2-NADP-ME (*nadpme-III* gene, GRMZM5G886257), which have not been characterized until present. Computational sorting prediction programs (ChloroP V1.1 and TargetP Server v1.01; Emanuelsson et al. 1999, 2000) indicate that neither Zmcyt2-NADP-ME nor Zmcyt1-NADP-ME contain any predictable straightforward organelle sorting signal. Malic enzyme genes are distributed in three chromosomes of maize: *nadpme-IVc* and *nadpme-II* in chromosome 3, *nadpme-IVa* and *nadpme-III* in chromosome 6, and *nadpme-I* in chromosome 8. *In silico*, studies of the gene sequences show that genes of plastidic enzymes have 20/19 exons/introns and genes of cytosolic enzymes have 19/18 exons/introns with the exception of *nadpme-III* (Zmcyt2-NADP-ME protein) that has eight exons and seven introns (Fig. 1a).

A multiple alignment of all maize NADP-ME predicted protein sequences show that they contain all five conservative motives previously defined for NADP-MEs (Fig. 1a, Drincovich et al. 2001) and pair identities >63 % (Fig. 1b). The plastidic isoforms share 84 % identity, while ZmC_4-NADP-ME is only 63 and 64 % identical to Zmcyt1- and Zmcyt3-NADP-ME, respectively. These values suggest a more recent divergence of the plastidic isoform genes. In addition, all maize isoforms were included in a phylogenetic tree constructed with a larger number of plant NADP-ME sequences than previously used (Fig. 2; Drincovich et al. 2001; 2010). The tree topology shows that Group III,

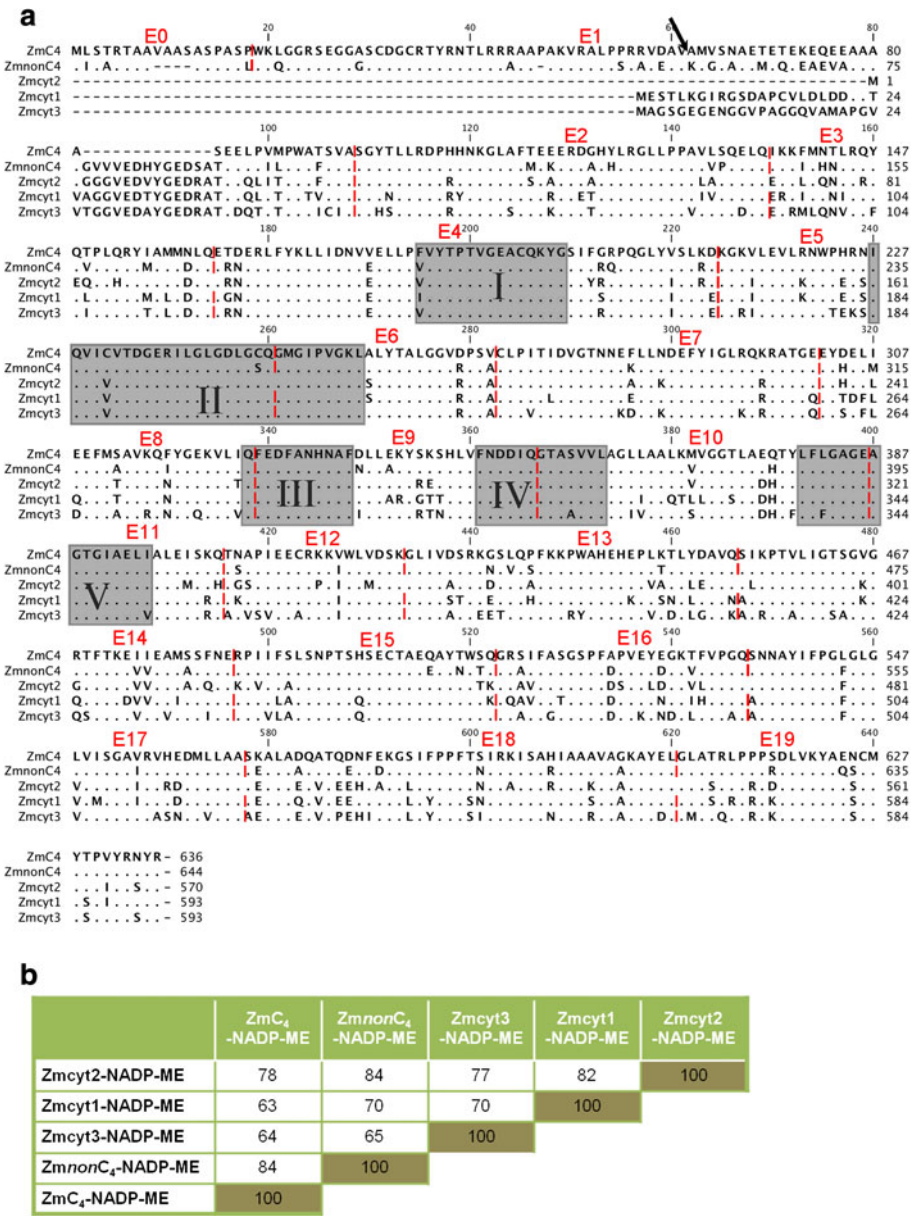

b

	ZmC_4 -NADP-ME	$Zmnon C_4$ -NADP-ME	Zmcyt3 -NADP-ME	Zmcyt1 -NADP-ME	Zmcyt2 -NADP-ME
Zmcyt2-NADP-ME	78	84	77	82	100
Zmcyt1-NADP-ME	63	70	70	100	
Zmcyt3-NADP-ME	64	65	100		
$Zmnon C_4$-NADP-ME	84	100			
ZmC_4-NADP-ME	100				

Fig. 1 **a** Alignment of the predicted amino acid sequences of all family members of *Zea mays* NADP-MEs. Conserved sequences found in all plant NADP-ME (sites I–V) are highlighted in *gray*. Fragments encoded in different exons are delimited by marks and numbered from E0 to E19, except for Zmcyt2-NADP-ME that has eight exons. The transit peptide processing site of ZmC_4- and Zm*non*C_4- is indicated with a *black arrow*. The access numbers to GenBank of each sequence are: J05130 (ZmC_4-NADP-ME); AY315822 (Zm*non*C_4-NADP-ME); AY864063 (Zmcyt3-NADP-ME); AY104511 (Zmcyt1-NADP-ME); and NM_001157493 (Zmcyt2-NADP-ME), **b** sequence identity (%) among *Zea mays* NADP-MEs

which previously included all monocot NADP-MEs (Drincovich et al. 2010) is now further divided into groups IIIA, IIIB, and IIIC, holding Zmcyt1-, Zmcyt2-, and plastidial NADP-MEs (ZmC_4- and Zm*non*C_4-), respectively (Fig. 2), in an arrangement similar to that obtained by Christin et al. (2009) based on gene sequences. On the other hand, Zmcyt3-NADP-ME is included in Group IV, composed of NADP-MEs from both mono and dicot species, as previously shown (Drincovich et al. 2010).

Expression patterns of NADP-ME genes in maize plants

The first approach to investigate the roles of uncharacterized maize NADP-MEs was to compare the expression of their genes in different organs. Thus, quantitative real-time polymerase chain reaction (qRT-PCR) experiments were performed with cDNAs from different maize samples, including leaf blades (L), stems (St), and roots (R), of 15-days seedlings; leaf sheaths (Sh), immature organs such as tassels (T), and ears (E) of mature plants (6–8 weeks old); and 14 DAP grains (G) (see "Methods" section). All NADP-ME transcripts, indicated hereinafter in italics to facilitate the interpretation of the results, showed different patterns of expression in these organs (Fig. 3a, Supplemental Fig. 1). With regards to the plastidic NADP-ME coding transcripts, *ZmC_4-NADP-ME* was most abundant in photosynthetic organs such as sheaths and blades of leaves, showing up to 800- and 2,150-fold higher levels in relation to other maize samples, respectively (Fig. 3a). On the other

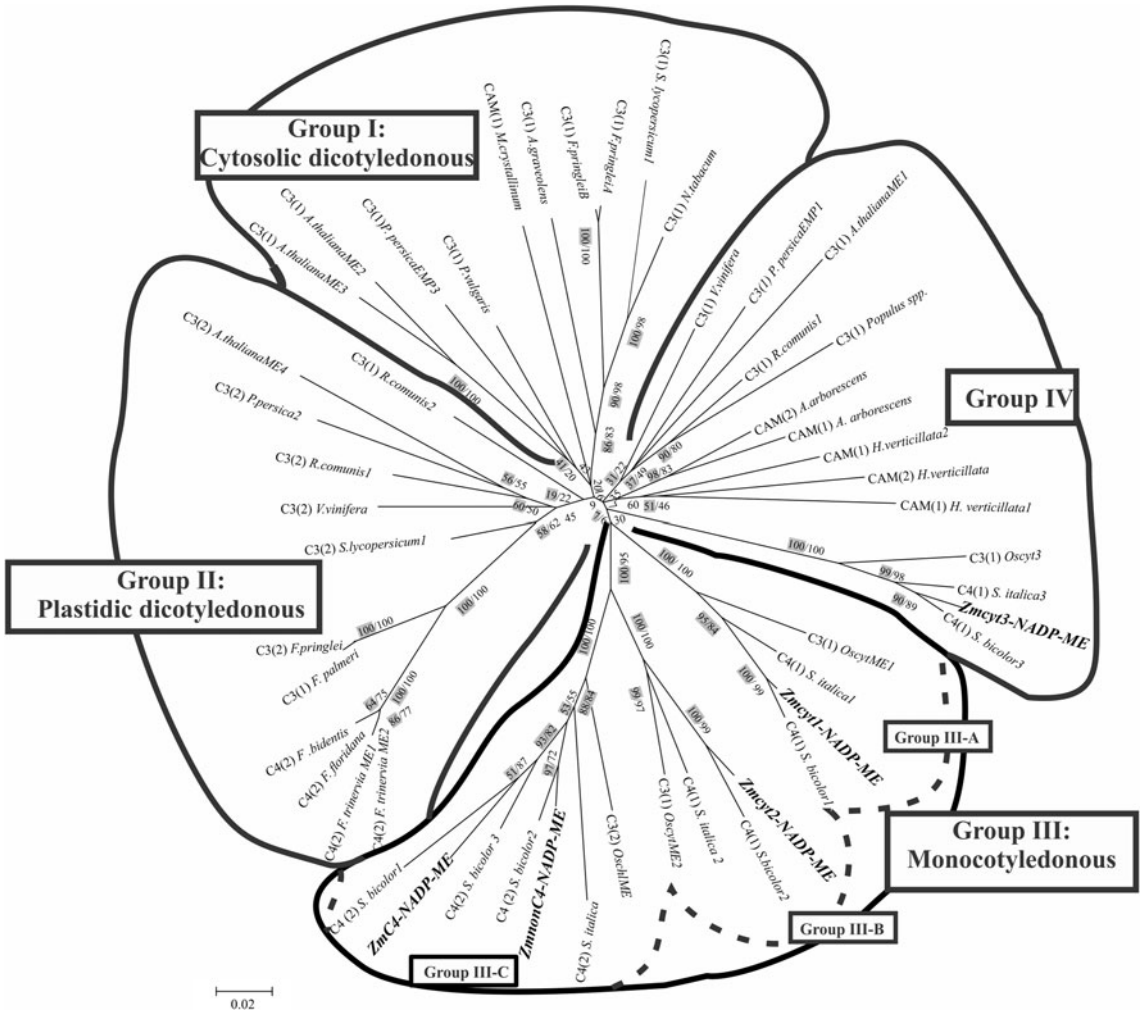

Fig. 2 Phylogenetic tree of plant NADP-ME isoforms. Mature proteins were aligned using Mega 5.10 and the phylogenetic tree was constructed by neighbor joining method (NJ). The tree topology shows four main groups: group I, cytosolic dicotyledonous; group II, plastidic dicotyledonous; group III, monocotyledonous; and group IV, including both mono and dicot NADP-MEs. The nomenclature used for each enzyme includes the photosynthetic type (CAM, C_3 or C_4) followed by a *number* which indicates the subcellular localization of each enzyme (1 for cytosolic and 2 for plastidic; Drincovich et al. 2001). *Branch numbers* indicate the statistical significance by neighbor joining (in *gray*) and maximum parsimony (in *white*)

hand, although *ZmnonC$_4$-NADP-ME* did not show such a great variations in expression levels among the samples, it reached significant higher levels in immature tassels and ears, in relation to sheaths and blades of leaves, grains, and roots (Fig. 3a). In the case of *Zmcyt1-NADP-ME,* it mostly accumulates in roots, showing around 80 times more abundance in this organ and up to 40 times in leaves and stems compared to grains (Fig. 3a). *Zmcyt2-NADP-ME* accumulates around 20 times more in leaf sheaths, roots, immature tassels, and immature ears than in grains (Fig. 3a). Finally, *Zmcyt3-NADP-ME* shows the greatest level in grains, where is up to 400-fold higher than in stems (Fig. 3a).

From the above results, it is deduced that the relative abundance of each NADP-ME transcript is different among the maize samples analyzed. For example, in leaves, the plastidic and cytosolic NADP-ME transcripts that predominate are *ZmC$_4$-* and *Zmcyt1-*, in roots *ZmnonC$_4$-* and *Zmcyt1-*, and in grains *ZmnonC$_4$-* and *Zmcyt3-NADP-ME*, which implies that different combinations of isoforms support the different metabolisms carried on by the organs analyzed (Fig. 3b).

Zmcyt3- and ZmnonC$_4$-NADP-ME show different expression profiles during grain development

Zmcyt3- and *ZmnonC$_4$-NADP-ME* expression was also compared in grains at different developmental stages. The samples were collected at four times after pollination, which were representative of the developing stages of cellular proliferation (7 days after pollination, DAP), reserves accumulation in the endosperm (14 and 20 DAP)

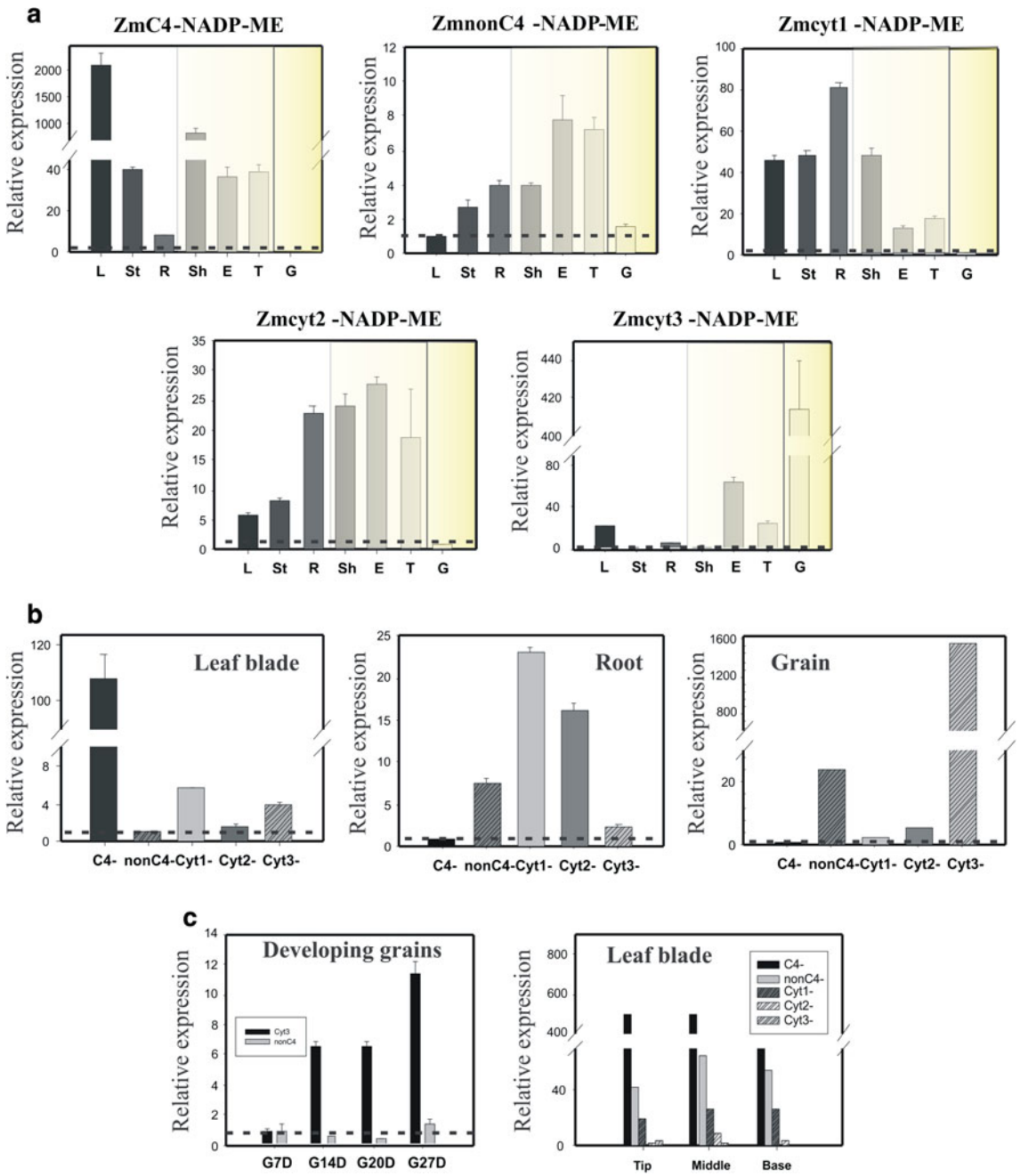

Fig. 3 Expression analysis of the five transcripts of NADP-ME in maize. **a** Relative expression of maize *NADP-MEs* in different organs. Analyses were made with RNA isolated from maize leaf blades (L); stems (St); roots (R); leaf sheaths (Sh); immature tassels (T); immature ears (E), and immature grains (G). *Y axis* refers to the fold difference in a particular transcript level relative to the sample in which the transcript shows the lowest expression: G for *ZmC*$_4$-, *Zmcyt1*-, and *Zmcyt2-NADP-ME*; L for *ZmnonC*$_4$*-NADP-ME*; and St for *Zmcyt3-NADP-ME*. The means and standard deviations of the results obtained using three independent RNAs as templates are shown. Each reaction was normalized using the C_t values corresponding to maize *actin1*. The different *colored backgrounds* indicate that maize plants at different stages of development were used to obtain the corresponding samples (see "Methods" section). **b** Relative expression levels of *NADP-ME* in leaves, roots and grains. The fold differences are relative to the transcript that shows the lowest expression in each organ: nonC4- in leaf blade; and C4- in root and grain. Short names for each transcript were used: C4- for *ZmC*$_4$*-NADP-ME*; nonC4- for *ZmnonC*$_4$*-NADP-ME*; Cyt3- for *Zmcyt3-NADP-ME*; Cyt1- for *Zmcyt1-NADP-ME* and Cyt2- for *Zmcyt2-NADP-ME*. **c** *ZmnonC*$_4$*-NADP-ME*, and *Zmcyt3-NADP-ME* levels in developing grains. The relative expression of *Zmcyt3-EM-NADP* (*gray*) and *ZmnonC*$_4$*-NADP-ME* (*black*) in grains at different times after pollination (7, 14, 20, and 27 DAP) are shown with respect to the corresponding level at 7 DAP. **d** Expression studies of NADP-ME transcripts along mature maize leaf blades. The expression levels of all *NADP-MEs* were evaluated in three fragments of a mature leaf blade: tip, middle, and base. Data correspond to the expression of each transcript in different segments in relation to the expression corresponding to the reference gene (maize *actin1*). Data represent the mean (±SD) of at least three independent assays

and maturation, and desiccation (27 DAP) (Liu et al. 2008) (Fig. 3c). Varying expression patterns of these two transcripts were obtained during the different stages of maize grains development. While *ZmnonC$_4$-NADP-ME* showed a twofold decrease from 7 to 20 DAP and then an increase to similar values found at 7 DAP, *Zmcyt3-NADP-ME* level increased 7 times from 7 to 14 DAP, followed by a second increase (70 % approximately) from 20 to 27 DAP, reaching almost 12-fold increase from the first to the final developmental stages analyzed (Fig. 3c).

NADP-ME transcripts levels along maize mature leaves

Expression levels of the transcripts from the complete NADP-ME family were assayed in the tip, the middle, and the base of maize fully expanded leaf blades. Different sections from maize leaves have shown different transcriptomes, in correlation with different photosynthetic metabolism and anatomy (Pick et al. 2011; Li et al. 2010). In our analysis, *ZmC$_4$-NADP-ME* levels increased from the base to the tip, while no important variations were observed for the second plastidic NADP-ME, *ZmnonC$_4$-NADP-ME* (Fig. 3d). On the other hand, the two major cytosolic NADP-ME transcripts (*Zmcyt1-NADP-ME* and *Zmcyt2-NADP-ME*) decreased from the middle part to the tip of the maize blade (Fig. 3d).

NADP-ME genes response to stress treatments in different maize organs

Several studies have reported that plant NADP-MEs respond to diverse stress conditions (recently reviewed by Doubnerová and Ryšlavá 2011). In this study, we selected five treatments to simulate different environmental conditions: high altitudes and/or high sun-light irradiance (UV-light treatment), alkaline soils (roots immersion in pH 8 or pH 11 solutions), pathogens attack (cellulase treatment), and drought (abscicic acid treatment). The expression profiles under these stress treatments were analyzed for all *NADP-MEs* in three organs of maize 15-days seedlings: leaves, stems, and roots (Fig. 4).

After the treatments, plastidic NADP-ME transcripts showed differential responses in leaves (Fig. 4a). *ZmC$_4$-NADP-ME* was induced 3–6 times by alkaline treatments, UV and ABA (Fig. 4a), while *ZmnonC$_4$-NADP-ME* was induced around 2–3 times with all treatments except pH 8 solution (Fig. 4a). Considering that *Zmcyt1-NADP-ME* is the most abundant transcript among the cytosolic NADP-MEs in leaves (Fig. 3b), it is important to notice its nearly fourfold induction with ABA and cellulase treatments (Fig. 4a). In stems, the most abundant plastidic transcript, *ZmnonC$_4$-NADP-ME* showed around sixfold induction under pH 11 treatment (Fig. 4b), while its counterpart most abundant cytosolic transcript, *Zmcyt1-NADP-ME* showed between 2 and 4 times induction with UV, pH 11, and ABA treatments, respectively (Fig. 4b). ABA and alkaline treatments in roots increased *ZmnonC$_4$-NADP-ME* expression around 2–4 times (Fig. 4c), while pH 11 and ABA generated the major induction effects in *Zmcyt1-NADP-ME* levels (Fig. 4c). In this organ, it is remarkably the almost 90-fold induction of *Zmcyt3-NADP-ME* by ABA treatment, which could turn this transcript into the most important under this condition.

Expression and characterization of Zmcyt1- and Zmcyt2-NADP-ME

Two uncharacterized NADP-ME genes were identified in the genome of *Zea mays*, which encode Zmcyt1- and Zmcyt2-NADP-ME. Both full-length cDNAs were amplified by reverse transcription (RT) from maize total RNA from leaves. The analyses of the predicted sequence of Zmcyt1-NADP-ME using the TIS Miner program (http://dnasminer.bic.nus.edu.sg/; Liu et al. 2005) found four possible ATG initiation sites. However, secondary structure stability programs (Vienna RNA Website, http://rna.tbi.univie.ac.at/cgi-bin/RNAfold.cgi; Hofacker 2003) and alignment to orthologs sequences showed that the most probable translation initiation site corresponds to the forth ATG (Fig. 1a). Thus, Zmcyt1-NADP-ME characterization was performed considering the sequence from this site (Fig. 1a). The deduced Zmcyt1- and Zmcyt2-NADP-ME proteins have molecular masses estimated around 66 and 63 kDa, similar to other NADP-MEs already characterized (Saigo et al. 2004; Detarsio et al. 2003). Both Zmcyt1- and Zmcyt2-NADP-MEs were successfully expressed in *E. coli* BL21(DE3) and purified to homogeneity using the same procedure described in this article (Detarsio et al. 2003), and proteins with the expected molecular masses were obtained (not shown). The kinetic characterization of Zmcyt1- and Zmcyt2- showed affinity constants for the substrates malate and NADP similar to that obtained for ZmC$_4$-NADP-ME (Table 1). However, around 1,500 and 70 times lower maximum catalytic activities (*k*cat) than the photosynthetic isoform were obtained for Zmcyt1- and Zmcyt2-NADP-ME, respectively (Table 1).

Conservative putative transcription factor binding sites across orthologs of maize NADP-ME genes

In order to detect relevant putative regulatory elements in maize NADP-ME genes, we performed an evolutionary based search of transcription factor binding motifs (TFBS), which is known as phylogenetic footprinting (Wasserman and Sandelin 2004). First, orthologs of each maize NADP-ME gene were identified in sorghum, *Setaria italica* and

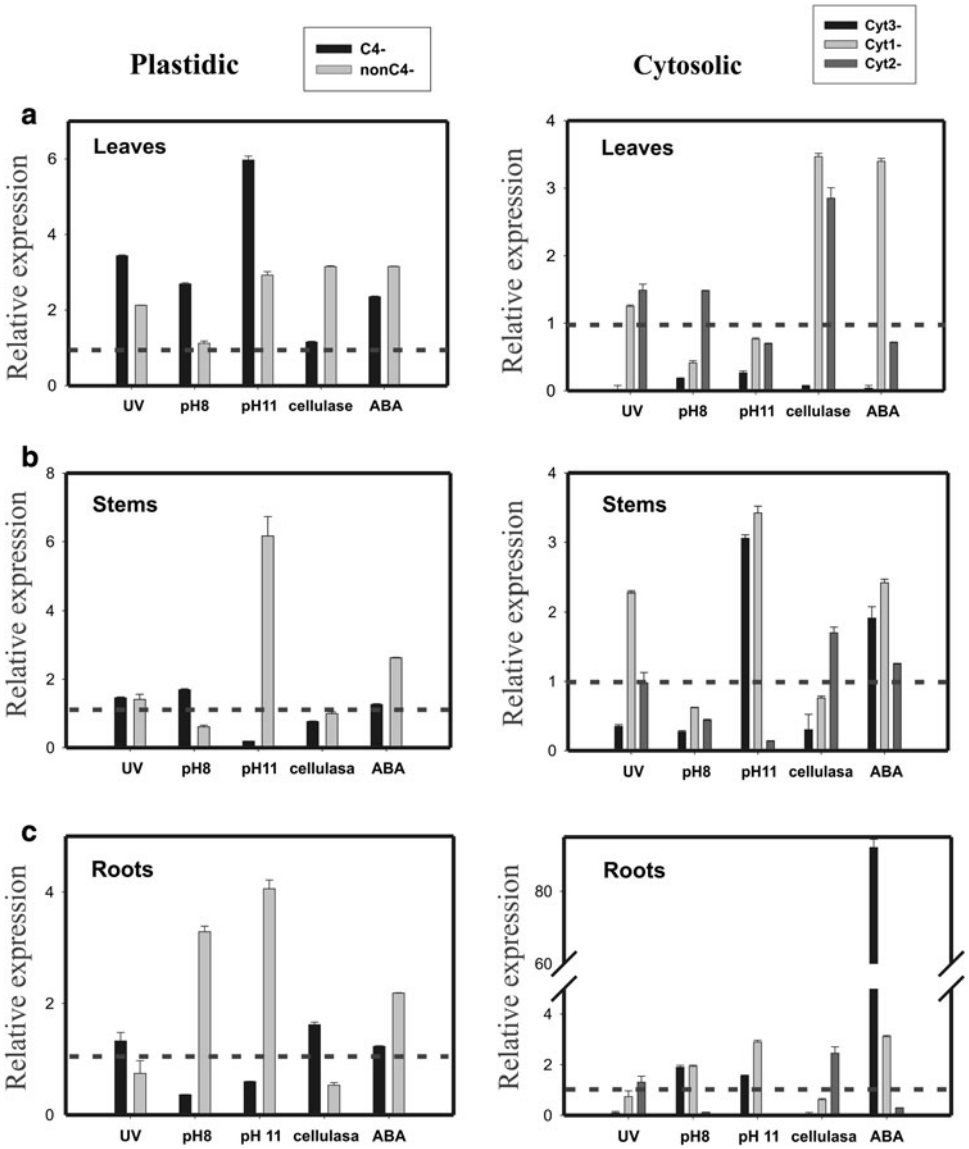

Fig. 4 Expression levels of NADP-ME transcripts in leaves (**a**), stems (**b**), and roots (**c**) under stress conditions. *Y axis* refers to the fold difference in a particular transcript level relative to the level found in control conditions. The means of the results obtained, using at least three independent RNAs as a template are shown. Each reaction was normalized using the C_t values corresponding to maize *actin1* mRNA. The abscissa indicates the abbreviation corresponding to the treatments applied: UV (2 W m^{-2} UV-light); pH 8 (60 mM $NaHCO_3$ pH 8.0); pH 11 (30 mM Na_2CO_3 pH 11.0); cellulase (0.5 % w/v cellulase); and ABA (250 μM abscisic acid)

Table 1 Comparative summary of the most important biochemical characteristics of the five NADP-ME family members

	ZmC$_4$-	Zm*non*C$_4$-	Zmcyt1-	Zmcyt2-	Zmcyt3-
*k*cat (s^{-1})	201.3 ± 9.8	105.6 ± 8.9	0.13 ± 0.02	3.0 ± 0.02	53.1 ± 2.8
Km malate (mM)	0.22 ± 0.02	0.42 ± 0.03	0.28 ± 0.04	0.18 ± 0.02	1.4 ± 0.6
Km NADP (μM)	8.0 ± 0.3	70.2 ± 0.3	9.9 ± 0.3	8.3 ± 0.02	19.1 ± 0.5
Monomer molecular mass (KDa)	62	64	66	63	66
Intracellular location	Plastidic	Plastidic	Cytosolic	Cytosolic	Cytosolic

The kinetic values are the average of at least three different determinations ±SD. Data were fit to a typical Michaelis–Menten equation with regression coefficients above 95 %. The kinetic parameters of Zmcyt3-NADP-ME (Detarsio et al. 2008) and maize plastidic NADP-MEs, at optimum pH, are included for comparison (Detarsio et al. 2003; Saigo et al. 2004)

rice (Table 2). Besides protein sequence similarity and syntheny (not shown), each group of orthologs showed the same exon–intron pattern (Fig. 2; Christin et al. 2009). Then, each group of orthologous sequences was aligned followed by a search of conserved TFBS (Ovcharenko et al. 2005). This approach is useful in eliminating false positives, and thus strengthening and simplifying the results (Wasserman and Sandelin 2004). Accordingly, in all the cases more than 200 putative TFBS were detected in each individual gene, but the lists were drastically reduced

Table 2 NADP-ME genes groups defined by orthologs or genes with similar function

	Cyt1- group	Cyt2- group	Cyt3- group	C_4- group	nonC_4- group
Z. mays	GRMZM2G159724	GRMZM5G886257	GRMZM2G118770	GRMZM2G085019	GRMZM2G122479
S. bicolor	Sb03g033250	Sb09g005810	Sb03g034280	Sb03g003230	Sb09g017550
S. italica	Si000774	Si021600	Si000808	Si000645	–
O. sativa	Os01g52500	Os05g09440	Os01g54030	–	Os01g09320

Cyt1-, *Cyt2-*, and *Cyt3- groups* includes orthologs from *Z. mays*, *S. bicolor*, *S. italica and O. sativa*, respectively. C4 and *non*C4 groups have a common evolutionary origin but were separated according to their physiological functions. Si000645 is included in the C4- group because, the product of this gene is involved in C4 photosynthesis; however the phylogenetic footprinting studies show more conserved TFBS with the non C4- group

when only those TFBS conserved among orthologs were considered (Fig. 5; Supplemental Table 1, 2).

In Zmcyt1- and Zmcyt3-NADP-ME genes, several conserved TFBS were detected, all of them in the promoter regions proximal to the transcription start site (TSS) (Fig. 5; Supplemental Table 1, 2). However, the analysis of Zmcyt2-NADP-ME did not return any conserved TFBS among the orthologous sequences (Table 2). The analyses of ZmC_4- and Zm*non*C_4-NADP-ME genes were more complex, although sorghum (Sb) has orthologs for both genes, *S. italica* (Sichl) and rice (Oschl) have only one plastidial NADP-ME-coding gene (Table 2). In the case of *S. italica*, this gene is involved in C_4 photosynthesis (Watson and Dallwitz 1992) then the sequence comparison of ZmC_4- was initially performed using SbC_4 and Sichl. When using ZmC_4-, SbC_4, and Sichl, only two conserved ERF2 binding sites were detected; however, if Sichl gene is excluded from the analysis, then fourteen conserved TFBS are detected (Fig. 5; Supplemental Table 1, 2). It is interesting to note that in ZmC_4- nine TFBS are located in introns while only three TFBS are in the promoter (Fig. 5). Besides, Zm*non*C_4- was compared with Sb*non*C_4- and Oschl (Table 2) since their function in plastids is non-photosynthetic. Several conserved TFBS in the promoter regions proximal to TSS and one within the 5′UTR sequence were detected (Fig. 5; Supplemental Table 1, 2). As Sichl did not show conserved TFBS with the photosynthetic genes (ZmC_4- and SbC_4), a search for conserved TFBS using the nonphotosynthetic genes (ZmnonC_4-, SbnonC_4- and Oschl) were performed. Interestingly, in this last case, several conserved TFBS were detected (Supplemental Table 1), which could be related with a more close evolution pattern with these genes.

A central assumption in phylogenetic footprinting is that the regulation of orthologous genes will be controlled by the same regulatory mechanisms in different species due to conserved functions. Then, to further investigate the regulation of NADP-ME genes, we searched for transcription factors (TF) coexpressed with rice NADP-ME genes that share putative TFBS with maize genes: Oscyt1, Oscyt3, and Oschl (Supplemental Table 3). RiceFREND is a gene coexpression database based on a large collection of microarray data derived from various rice tissues at different stages of growth and development under natural field conditions or treated with phytohormones (Sato et al. 2013). Some TF that putatively bind to the TFBS previously detected were found among the coexpressed genes with mutual ranks (MR) below 1,000, which indicates a strong correlation (Supplemental Table 3; Obayashi et al. 2009; Obayashi and Kinoshita 2010). The expression pattern of Oscyt1 is highly similar to ERF2 and PIF3, for which the binding sites were located within the promoter region of this gene (Fig. 5; Supplemental Table 1, 2). This indicates that these two TF could be important regulators of the expression of cyt1- genes. Oscyt3 is coexpressed with several TF of the bZIP family (Supplemental Table 3). Accordingly, in the promoter of cyt3- genes, several bZIP TFBS were detected (Fig. 5; Supplemental Table 1, 2) which indicate that they are highly regulated by this TF family probably in response to ABA. On the other hand, only one bZIP TF (ABI5) was coexpressed with Oschl albeit many bZIP TFBS were detected (Fig. 5; Supplemental Table 2, 3).

Discussion

The presence of three genes for cytosolic NADP-MEs are highly conserved among species with either C_3 or C_4 photosynthetic carbon metabolism

Three maize genes encoding putative cytosolic NADP-MEs are presented in this study, which display different pattern of organ expression (Fig. 3), response to stress stimuli (Fig. 4) and biochemical properties (Table 1). Previous study has demonstrated good correlation between transcript and protein abundance in maize (Liu et al. 2011), which supported the consideration of transcript amount as an indicative of the amount of the corresponding protein (Pick et al. 2011). *Zmcyt1-* and *Zmcyt2-NADP-ME* are expressed in practically all maize organs analyzed, presenting the lowest levels in grains, where *Zmcyt3-NADP-*

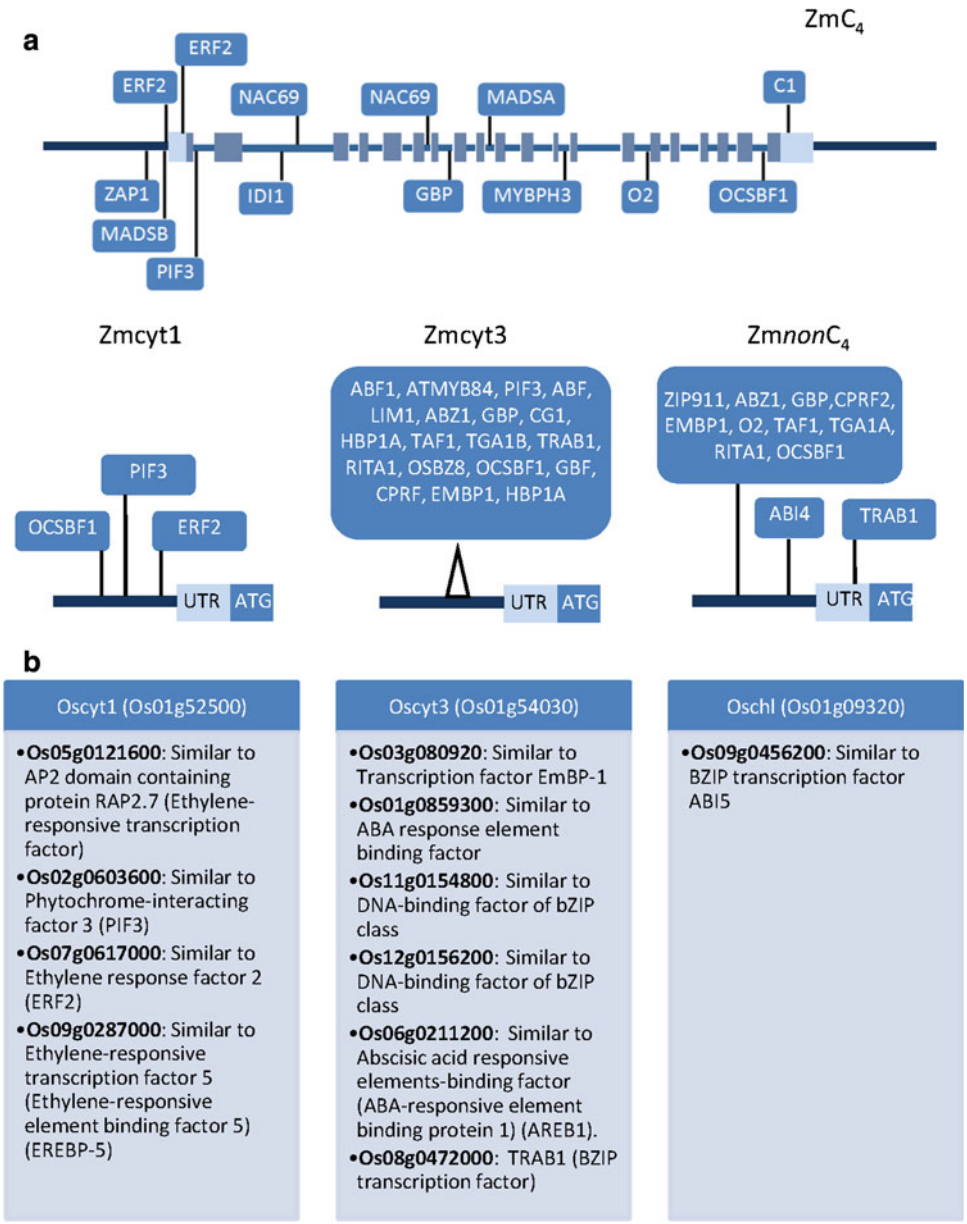

Fig. 5 Multi-conserved transcription factor binding sites. **a** The transcription factor binding sites (TFBS) evolutionarily conserved across maize, sorghum, *S. italica*, and rice were detected by Mulan and MultiTF web tools. The TFBS shown for ZmC_4 are shared with SbC_4 and absent in $nonC_4$ genes. *Dark boxes* indicate exons and *light boxes* indicate untranscribed regions. Zmcyt1-, Zmcyt2-, and Zmcyt3- gene sequences were compared with their corresponding orthologs. Zm*non*C_4 was compared with Sb*non*C_4 and OschlME. **b** Rice coexpressed transcription factor genes that could bind to the TFBS detected. The genes from *O. sativa* that share evolutionary conserved TFBS with maize genes were analyzed with RiceFREND web tool. The complete outputs of MULAN/MultiTF and RiceFREND analyses are included in Supplemental Table 1 and 2, respectively

ME displays the highest level of expression (Fig. 3). However, although the overlapping distribution of *Zmcyt1*- and *Zmcyt2-NADP-MEs* throughout maize organs, they respond differentially to stress situations (Fig. 4). *Zmcyt1NADP-ME* increases in leaves after cellulose and ABA treatment and in stems after root alkalinisation and UVB treatment (Fig. 4). On the other hand, *Zmcyt2-NADP-ME* increases in leaves, stems, and roots after cellulose treatment (Fig. 4). With regards to *Zmcyt3-NADP-ME*, apart from the almost exclusive expression in grains, distinct response to stress treatments than that shown by the other cytosolic NADP-MEs was found (Fig. 4). In particular, *Zmcyt3-NADP-ME* expression seems to be controlled by ABA, as indicated by its important induction by ABA treatment in roots (Fig. 4) and the presence of several and conserved ABA-response elements in its promoter (Fig. 5). Maize seed development is strongly controlled by ABA mainly by mean of the control of starch, protein, and lipids synthesis (Liu et al. 2008). In this way, Zmcyt3-NADP-ME could be supplying carbon and reducing power for those biosynthetic processes, in accordance to its distinct biochemical properties (Table 1; Detarsio et al. 2008).

In the present study, orthologs for the three maize cytosolic NADP-ME were identified in related C_3 and C_4 monocots (Table 2). In particular, cyt1 and cyt3 NADP-ME-groups seem to be controlled by similar regulatory mechanisms in monocots, which reinforces the idea of conserved functions for the orthologs of these groups (Table 2; Fig. 5). In the case of cyt2-NADP-ME group, although orthologs were detected in monocots (Table 2),

no conserved TFBS were identified. This could be due to the lack of information about TFBS for this gene, the binding to farther regions not analyzed here or to the lack of conservation of the regulatory mechanisms due to the diversification of function across the species analyzed. However, it is noticeable that the presence of three cytosolic NADP-MEs is also the case in the dicot model plant species *A. thaliana* (Gerrard Wheeler et al. 2005; Maurino et al. 2009). Thus, the presence of three genes encoding cytosolic NADP-MEs seem to be a conserved feature among both related and distant plant species with different photosynthetic metabolism.

Two plastidic NADP-MEs, is it a feature specific for all C_4 species?

Regarding the two maize plastidic NADP-MEs, *ZmC$_4$-NADP-ME* is practically exclusive of photosynthetic organs, while *ZmnonC$_4$-NADP-ME* is found in all the organs analyzed, especially in nonphotosynthetic organs (Fig. 3). *ZmnonC$_4$-NADP-ME* responds to several different stress treatments and in different organs (Fig. 4), which is in accord with previous study that pointed out this isoform as a stress-responsive enzyme (Maurino et al. 2001). The well-distinct biochemical and kinetic properties of the two plastidic ZmNADP-MEs (Alvarez et al. 2012; Saigo et al. 2013), along with the different organ distribution and stress responsive expression (Fig. 3, 4) reinforces the important, but particular role that each plastidic isoform fulfils in vivo. Several conserved TFBS were detected in the orthogues encoding nonphotosynthetic plastidic isoforms from sorghum and rice (Table 2; Fig. 5) suggesting conserved roles in both C_3 and C_4 species. Moreover, a nonphotosynthetic NADP-ME may fulfil an essential metabolic role in plastids of nonphotosynthetic organs, e.g., in the generation of reductive power and/or pyruvate, as indicated by the presence of such an enzyme in distant plant species (Drincovich et al. 2001; Maurino et al. 2009).

With regards to *ZmC$_4$-NADP-ME*, its expression level correlates with the occurrence of the C_4 cycle, increasing from the base to the tip of the leaf blade (Fig. 3; Pick et al. 2011). Within the leaf blade, ZmC$_4$-NADP-ME is compartmentalized to bundle sheath chloroplast (Maurino et al. 1997). Although the high *ZmC$_4$-NADP-ME* levels detected in maize leaf, an induction of *ZmC$_4$-NADP-ME* was detected after treatments with UVB or high pH (Fig. 4). Previous study has shown UVB-induction of ZmC$_4$-NADP-ME, which was linked to higher energy demand for membrane repair (Drincovich et al. 1998). Moreover, among the several conserved TFs that putatively regulate *ZmC$_4$-NADP-ME* expression (Fig. 5), PIF3 is particularly interesting because it accumulates under UV-light treatment (Heim et al. 2003), and is necessary for early chloroplast greening and rapid light-induced expression of nuclear genes encoding chloroplast components (Monte et al. 2004). In addition, PIF3 transcript (GRMZM2G062541) is more abundant in BSC than in MC (Chang et al. 2012), which suggests that it may be implicated in the transduction of the light signal that induces the transcription of ZmC$_4$- gene during maize chloroplast greening. On the other hand, *ZmC$_4$-NADP-ME* expression is also modified by other stress treatments, as alkaline stress treatments of roots, which may reflect an overall response for higher demand of photosynthetic products. Thus, the C_4 specific NADP-ME represents a highly expressed isoform in photosynthetic organs, which presents a fine tune of regulation controlled by several TF and response to stress treatments. Notably, and contrary to other NADP-ME genes, the majority of the TFBS in ZmC$_4$-gene are located in the introns and not in the promoter (Fig. 5).

The search of orthologs of the maize plastidic NADP-ME genes indicated that while sorghum presents also two plastidic NADP-MEs with conserved TFBS, *S. italica* shows only one (Table 2). Moreover, practically no TFBS conservation between Sichl-NADP-ME gene and the photosynthetic NADP-MEs from maize and sorghum genes were detected. However, several conserved TFBS were detected in the comparison with nonphotosynhtetic NADP-MEs from maize, sorghum, and rice (Supplemental Table 1). Although these results seem to contradict the photosynthetic role of Sichl-NADP-ME, it could be explained by the independent evolutionary origin of C_4 photosynthesis in Setaria and maize–sorghum lineages, which could manage different regulation programs to set the expression of C_4 genes (Sage and Zhu 2011). Moreover, Setaria belongs to a particular monocot lineage in which species with different decarboxylating enzymes were detected (Sage and Zhu 2011). Considering the results obtained, it would be interesting to perform the characterization of the plastidic NADP-ME from Setaria to compare its properties with other plastidic C_4 and non C_4 NADP-MEs and further study the expression pattern of its gene (Saigo et al. 2013).

Did the presence of a multigene family in combination with the biochemical plasticity of the NADP-ME isoforms facilitate the appearance of the NADP-ME recruited for the C_4 cycle?

The most successful agricultural C_4 crops species have arisen from the NADP-ME type mechanism (maize, sorghum, sugarcane, switchgrass, among others), providing at least circumstantial evidence for the superiority of this pathway (Furbank 2011). It has been discussed in several reviews that the C_4 NADP-ME mechanism might provide an advantage because decarboxylation occurs within the

BS chloroplasts, the site of refixation by RuBisCO, avoiding any leakiness of the bundle sheath to CO_2 (von Caemmerer and Furbank 2003). However, it is a matter of actual debate why this type of C_4 cycle is more distributed than the others. In this sense, among the decarboxylating enzymes which were recruited for the C_4 pathway, multigene families are detected in the case of NADP-ME, and particular roles have been attributed to each member (Maurino et al. 2009). Besides, NADP-ME is an enzyme in which the change in just one or two amino acids can render a novel enzymatic form regulated in a different way, and thus, capable to fulfil novel physiological roles. This fact has been extensively proven for the *Arabidopsis* NADP-ME isoforms, where isoforms that share >90 % of protein identity are regulated in opposite ways or even behave differently in terms of reversibility (Gerrard Wheeler et al. 2008; 2009). Moreover, it has also been found that the physiological context of particular NADP-ME isoforms exerts accurate control of NADP-ME activity *in planta* (Arias et al. 2013). Overall, this plasticity shown by the NADP-ME makes us wonder if the presence of a multigene family, in which each gene encodes an isoform with particular biochemical properties due to minimal changes in the primary structure, would have facilitated the appearance of an enzyme well-suited to fulfil the requirements for an efficient C_4 mechanism. Whether this issue is related or not to the widespread distribution of the C_4 NADP-ME subtype should be proven.

Acknowledgments CSA, MFD and MS are members of the Researcher Career of Consejo Nacional de Investigaciones Científicas y Técnicas (CONICET, Argentina) and CEA and EM are fellows of the same institution. We thank Dr. Marcos A. Tronconi for the helpful discussion of sequence analysis. This study has been supported by National Agency for Promotion of Science and Technology (ANPCyT) and CONICET.

References

Alvarez CE, Detarsio E, Moreno S, Andreo CS, Drincovich MF (2012) Functional characterization of residues involved in redox modulation in maize photosynthetic NADP-malic enzyme activity. Plant Cell Physiol 53:1144–1153. doi:10.1093/pcp/pcs059

Arias CA, Drincovich MF, Andreo CS, Gerrard Wheeler MC (2013) Fumarate and cytosolic pH as modulators of the synthesis or consumption of C4 organic acids through NADP-malic enzyme in Arabidopsis thaliana. Plant Mol Biol 81:297–307

Aubry S, Brown NJ, Hibberd JM (2011) The role of proteins in C(3) plants prior to their recruitment into the C(4) pathway. J Exp Bot 62:3049–3059. doi:10.1093/jxb/err012

Casati P, Drincovich MF, Edwards GE, Andreo CS (1999) Malate metabolism through NADP-malic enzyme in plant defense. Photosynth Res 61:99–105. doi:10.1590/S0100-879X1999001000002

Chang Y-M, Liu W-Y, Shih AC-C, Shen M-N, Lu C-H, Lu M-YJ, Yang H-W, Wang TY, Chen SC, Chen SM, Li WH, Ku MS (2012) Characterizing regulatory and functional differentiation between maize mesophyll and bundle sheath cells by transcriptomic analysis. Plant Physiol 160:165–177. doi:10.1104/pp.112.203810

Chi W, Yang J, Wu N, Zhang F (2004) Four rice genes encoding NADP malic enzyme exhibit distinct expression profiles. Biosci Biotechnol Biochem 68:1865–1874. doi:10.1271/bbb.68.1865

Choi H, Hong J, Ha J, Kang J, Kim SY (2000) ABFs, a family of ABA-responsive element binding factors. J Biol Chem 275:1723–1730. doi:10.1074/jbc.275.3.1723

Christin P-A, Samaritani E, Petitpierre B, Salamin N, Besnard G (2009) Evolutionary insights on C_4 photosynthetic subtypes in grasses from genomics and phylogenetics. Genome Biol Evol 1:221–230

Cushman JC (1992) Characterization and expression of a NADP-malic enzyme cDNA induced by salt stress from the facultative crassulacean acid metabolism plant, *Mesembryanthemun crystallinum*. Eur J Biochem 208:259–266

de Pater S, Greco V, Pham K, Memelink J, Kijne J (1996) Characterization of a zinc-dependent transcriptional activator from arabidopsis. Nucl Acids Res 24:4624–4631. doi:10.1093/nar/24.23.4624

Detarsio E, Gerrard Wheeler MC, Campos Bermúdez VA, Andreo CS, Drincovich MF (2003) Maize C_4 NADP-malic enzyme. Expression in *Escherichia coli* and characterization of site-direct mutants at the putative nucleotide-binding sites. J Biol Chem 278:13757–13764. doi:10.1074/jbc.M212530200

Detarsio E, Alvarez CE, Saigo M, Andreo CS, Drincovich MF (2007) Identification of domains involved in tetramerization and malate inhibition of maize C_4 NADP-malic enzyme. J Biol Chem 282:6053–6060. doi:10.1074/jbc.M609436200

Detarsio E, Maurino VG, Alvarez CE, Müller GL, Andreo CS, Drincovich MF (2008) Maize cytosolic NADP-malic enzyme (ZmCytNADP-ME): a phylogenetically distant isoform specifically expressed in embryo and young root. Plant Mol Biol 68:355–367. doi:10.1007/s11103-008-9375-8

Doubnerová V, Ryšlavá H (2011) What can enzymes of C_4 photosynthesis do for plants under stress? Plant Sci 180:575–583

Drincovich MF, Casati P, Andreo CS, Donahue R, Edwards GE (1998) UV-B induction of NADP-malic enzyme in etiolated maize seedlings. Plant Cell Environ 21:63–70. doi:10.1046/j.1365-3040.1998.00240.x

Drincovich MF, Casati P, Andreo CS (2001) NADP-malic enzyme from plants: a ubiquitous enzyme involved in different metabolic pathways. FEBS Lett 490:1–6

Drincovich MF, Lara M, Maurino VG, Andreo C (2010) C_4 decarboxylases. Different solutions for the same biochemical problem, the provision of CO_2 in the bundle sheath cells. In: Raghavendra A, Sage RF (eds) C_4 photosynthesis and related CO_2 concentrating mechanisms. Springer, Heidelberg, pp 277–300

Eastmond PJ, Dennis DT, Rawsthorne S (1997) Evidence that a malate/inorganic phosphate exchange translocator imports carbon across the leucoplast envelope for fatty acid synthesis in developing castor seed endosperm. Plant Physiol 114:851–856. doi:10.1104/pp.114.3.851

Edwards GE, Walker DA (1983) C_3, C_4: mechanisms, and cellular and environmental regulation, of photosynthesis. Blackwell Scientific publications, Oxford

Emanuelsson O, Nielsen H, von Heijne G (1999) ChloroP, a neural network-based method for predicting chloroplast transit peptides and their cleavage sites. Protein Sci 8:978–984. doi:10.1110/ps.8.5.978

Emanuelsson O, Nielsen H, Brunak S, von Heijne G (2000) Predicting subcellular localization of proteins based on their N-terminal amino acid sequence. J Mol Biol 300:1005–1016. doi:10.1006/jmbi.2000.3903

Estavillo GM, Rao SK, Reiskind JB, Bowes G (2007) Characterization of the NADP malic enzyme gene family in the facultative, single-cell C_4 monocot *Hydrilla verticillata*. Photosynth Res 1:43–57. doi:10.1007/s11120-007-9212-y

Feller A, Machemer K, Braun EL, Grotewold E (2011) Evolutionary and comparative analysis of MYB and bHLH plant transcription factors. Plant J 66:94–116. doi:10.1111/j.1365-313X.2010.04459.x

Finkelstein RR, Wang ML, Lynch TJ, Rao S, Goodman HM (1998) The Arabidopsis abscisic acid response locus ABI4 encodes an APETALA2 domain protein. Plant Cell 10:1043–1054. doi:10.1105/tpc.12.4.599

Franke KE, Adams DO (1995) Cloning a full-length cDNA for malic enzyme (EC 1.1.40.) from grape berries. Plant Physiol 107:1009–1010. doi:10.1104/pp.107.3.1009

Furbank RT (2011) Evolution of the C(4) photosynthetic mechanism: are there really three C(4) acid decarboxylation types? J Exp Bot 62:3103–3108. doi:10.1093/jxb/err080

Fushimi T, Umeda M, Shimazaki T, Kato A, Toriyama K, Uchimiya H (1994) Nucleotide sequence of a rice cDNA similar to a maize NADP-dependent malic enzyme. Plant Mol Biol 24:965–967. doi:10.1007/BF00014450

Gerrard Wheeler MC, Tronconi MA, Drincovich MF, Andreo CS, Flügge U, Maurino VG (2005) A comprehensive analysis of the NADP-malic enzyme gene family of Arabidopsis. Plant Physiol 139:39–51. doi:10.1104/pp.105.065953.1

Gerrard Wheeler MC, Arias CL, Tronconi MA, Maurino VG, Andreo CS, Drincovich MF (2008) Arabidopsis thaliana NADP-malic enzyme isoforms: high degree of identity but clearly distinct properties. Plant Mol Biol 67:231–242. doi:10.1007/s11103-008-9313-9

Gerrard Wheeler MC, Arias C, Maurino VG, Andreo CS, Drincovich MF (2009) Identification of domains involved in the allosteric regulation of cytosolic *Arabidopsis thaliana* NADP-malic enzymes. FEBS J. 276:5665–5677. doi:10.1111/j.1742-4658.2009.07258.x

Goodstein DM, Shu S, Howson R, Neupane R, Hayes RD, Fazo J, Mitros T, Dirks W, Hellsten U, Putnam N, Rokhsar DS (2011) Phytozome: a comparative platform for green plant genomics. Nucl Acids Res 40:1–9. doi:10.1093/nar/gkr944

Gu Q, Ferrándiz C, Yanofsky MF, Martienssen R (1998) The FRUITFULL MADS-box gene mediates cell differentiation during *Arabidopsis* fruit development. Development 125:1509–1517

Hatch MD (1987) C_4 photosynthesis: a unique blend of modified biochemistry, anatomy and ultrastructure. Biochim Biophys Acta 895:81–106

Heim MA, Jakoby M, Werber M, Martin C, Weisshaar B, Bailey PC (2003) The basic helix-loop-helix transcription factor family in plants: a genome-wide study of protein structure and functional diversity. Mol Biol Evol 20:735–747. doi:10.1093/molbev/msg088

Hellemans J, Mortier G, De Paepe A, Speleman F, Vandesompele J (2007) qBase relative quantification framework and software for management and automated analysis of real-time quantitative PCR data. Genome Biol 8:R19. doi:10.1186/gb-2007-8-2-r19

Hobo T, Kowyama Y, Hattori T (1999) A bZIP factor, TRAB1, interacts with VP1 and mediates abscisic acid-induced transcription. PNAS 96:15348–15353. doi:10.1073/pnas.96.26.15348

Hofacker IL (2003) Vienna RNA secondary structure server. Nucleic Acids Res 31:3429–3431. doi:10.1093/nar/gkg599

Honda H, Shimada H, Akagi H (1997) Isolation of cDNA for an NADP-malic enzyme from *Aloe arborescens*. DNA Res 4:397–400. doi:10.1093/dnares/4.6.397

Honda H, Akagi H, Shimada H (2000) An isozyme of the NADP-malic enzyme of a CAM plant, *Aloe arborescens*, with variation on conservative amino acid residues. Gene 243:85–92

Izawa T, Foster R, Nakajima M, Shimamoto K, Chua NH (1994) The rice bZIP transcriptional activator RITA-1 is highly expressed during seed development. Plant Cell 6:1277–1287. doi:10.1105/tpc.6.9.1277

Jothi R, Cuddapah S, Barski A, Cui K, Zhao K (2008) Genome-wide identification of in vivo protein-DNA binding sites from ChIP-Seq data. Nucleic Acids Res 36:5221–5231. doi:10.1093/nar/gkn488

Katagiri F, Lam E, Chua NH (1989) Two tobacco DNA-binding proteins with homology to the nuclear factor CREB. Nature 340:727–730. doi:10.1038/340727a0

Kawaoka A, Kaothien P, Yoshida K, Endo S, Yamada K, Ebinuma H (2000) Functional analysis of tobacco LIM protein Ntlim1 involved in lignin biosynthesis. Plant J 22:289–301. doi:10.1046/j.1365-313x.2000.00737.x

Kunieda T, Mitsuda N, Ohme-Takagi M, Takeda S, Aida M, Tasaka M, Kondo M, Nishimura M, Hara-Nishimura I (2008) NAC family proteins NARS1/NAC2 and NARS2/NAM in the outer integument regulate embryogenesis in *Arabidopsis*. Plant Cell 20:2631–2642. doi:10.1105/tpc.108.060160

Lai LB, Tausta SL, Nelson TM (2002) Differential regulation of transcripts encoding cytosolic NADP-malic enzyme in C_3 and C4 *Flaveria* species. Plant Physiol 128:140–149. doi:10.1104/pp.010449

Langdale JA (2011) C_4 cycles: past, present, and future research on C_4 photosynthesis. Plant Cell 23:3879–3892. doi:10.1105/tpc.111.092098

Laporte MM, Shen B, Tarczynski MC (2002) Engineering for drought avoidance: expression of maize NADP-malic enzyme in tobacco results in altered stomatal function. J Exp Bot 3:699–705. doi:10.1093/jexbot/53.369.699

Lee J, Lee I (2010) Regulation and function of SOC1, a flowering pathway integrator. J Exp Bot 6:2247–2254. doi:10.1093/jxb/erq098

Li P, Ponnala L, Gandotra N, Wang L, Si Y, Tausta SR, Kebrom TH, Provart N, Patel R, Myers CR, Reidel EJ, Turgeon R, Liu P, Sun Q, Nelson T, Brutnell TP (2010) The developmental dynamics of the maize leaf transcriptome. Nat Genet 42:1060–1069. doi:10.1038/ng.7031060

Lipka B, Steinmüller K, Rosche E, Borsch D, Westhoff P (1994) The C_3 plant *Flaveria pringlei* contains a plastidic NADP-malic enzyme which is orthologous to the C_4 isoform of the C_4 plant *F. trinervia*. Plant Mol Biol 26:1775–1783. doi:10.1007/BF00019491

Liu W, Saint DA (2002) Validation of a quantitative method for real time PCR kinetics. Biochem Biophys Res Commun 294:347–353. doi:10.1016/S0006-291X

Liu H, Han H, Li J, Wong L (2005) DNAFSMiner: a web-based software toolbox to recognize two types of functional sites in DNA sequences. Bioinformatics 21:671–673. doi:10.1093/bioinformatics/bth437

Liu X, Fu J, Gu D, Liu W, Liu T, Peng Y, Wang J, Wang G (2008) Genome-wide analysis of gene expression profiles during the kernel development of maize (*Zea mays* L.). Genomics 91:378–387. doi:10.1016/j.ygeno.2007.12.002

López-Becerra E, Puigdomenech P, Stiefel V (1998) A gene coding for a malic enzyme expressed in the embryo root epidermis from *Zea mays* (Accession No. AJ224847) (PGR98-081). Plant Physiol 117:332

Maddaloni M, Donini G, Balconi C, Rizzi E, Gallusci P, Forlani F, Lohmer S, Thompson R, Salamini F, Motto M (1996) The transcriptional activator Opaque-2 controls the expression of a cytosolic form of pyruvate orthophosphate dikinase-1 in maize endosperms. Mol Gen Genet 250:647–654. doi:10.1007/s004380050117

Manoli A, Sturaro A, Trevisan S, Quaggiotti S, Nonis A (2012) Evaluation of candidate reference genes for qPCR in maize. J Plant Physiol 169:807–815. doi:10.1016/j.jplph.2012.01.019

Martinez-Garcia JF, Moyano E, Alcocer MJC, Martin C (1998) Two bZIP proteins from *Antirrhinum* flowers referentially bind a hybrid C-box/G-box motif and help to define a new sub-family of bZIP transcription factors. Plant J 13:489–505. doi:10.1046/j.1365-313X.1998.00050.x

Martinoia E, Rentsch D (1994) Malate compartmentation: responses to a complex metabolism. Annu Rev Plant Physiol Plant Mol Biol 45:447–467. doi:10.1146/annurev.pp.45.060194.002311

Maurino VG, Drincovich MF, Casati P, Andreo CS, Edwards GE, Ku MSB, Gupta SK, Franceschi VR (1997) NADP-malic enzyme: immunolocalization in different tissues of the C_4 plant maize and the C_3 plant wheat. J Exp Bot 48:799–811. doi:10.1093/jxb/48.3.799

Maurino VG, Saigo M, Andreo CS, Drincovich MF (2001) Nonphotosynthetic NADP-malic enzyme from maize: a constitutively expressed enzyme that responds to plant defense inducers. Plant Mol Biol 45:409–420. doi:10.1023/A:1010665910095

Maurino VG, Gerrard Wheeler MC, Andreo CS, Drincovich MF (2009) Redundancy is sometimes seen only by the uncritical: does Arabidopsis need six malic enzyme isoforms? Plant Sci 176:715–721. doi:10.1016/j.plantsci.2009.02.012

Mikami K, Sakamoto A, Iwabuchi M (1994) The HBP-1 family of wheat basic leucine zipper proteins interacts with overlapping & acting hexamer motifs of plant histone genes. J Biol Chem 269:9974–9985

Monte E, Tepperman JM, Al-Sady B, Kaczorowski KA, Alonso JM, Ecker JR, Li X, Zhang Y, Quail PH (2004) The phytochrome-interacting transcription factor, PIF3, acts early, selectively, and positively in light-induced chloroplast development. Proc Natl Acad Sci 101:16091–16098. doi:10.1073/pnas.0407107101

Mukherjee K, Choudhury AR, Gupta B, Gupta S, Sengupta DN (2006) An ABRE-binding factor, OSBZ8, is highly expressed in salt tolerant cultivars than in salt sensitive cultivars of indica rice. BMC Plant Biol 6:1–14. doi:10.1186/1471-2229-6-18

Müller D, Schmitz G, Theres K (2006) Blind homologous R2R3 Myb genes control the pattern of lateral meristem initiation in *Arabidopsis*. Plant Cell 18:586–597. doi:10.1105/tpc.105.038745

Müller GL, Drincovich MF, Andreo CS, Lara MV (2008) *Nicotiana tabacum* NADP-malic enzyme: cloning, characterization and analysis of biological role. Plant Cell Physiol 49:469–480. doi:10.1093/pcp/pcn022

Nakano T, Nishiuchi T, Suzuki K, Fujimura T, Shinshi H (2006) Studies on transcriptional regulation of endogenous genes by ERF2 transcription factor in tobacco cells. Plant Cell Physiol 47:554–558. doi:10.1093/pcp/pcj017

Ni M, Tepperman JM, Quail PH (1998) PIF3, a phytochrome-interacting factor necessary for normal photoinduced signal transduction, is a novel basic helix-loop-helix protein. Cell 95:657–667. doi:10.1016/S0092-8674(00)81636-0

Niu X, Guiltinan MJ (1994) DNA binding specificity of the wheat bZIP protein EmBP-1. Nucleic Acids Res 22(23):4969–4978. doi:10.1093/nar/22.23.4969

Obayashi T, Kinoshita K (2010) Coexpression landscape in ATTED-II: usage of gene list and gene network for various types of pathways. J Plant Res 123:311–319. doi:10.1007/s10265-010-0333-6

Oeda K, Salinas J, Chua NH (1991) A tobacco bZip trancription activator (TAF-1) binds to a G-box motif conserved in plant genes. EMBO J 10:1793–1802

Outlaw WH, Manchester J, Brown PH (1981) High levels of malic enzyme activities in *Vicia faba* L. epidermal tissue. Plant Physiol 68:1047–1051. doi:10.1104/pp.68.5.1047

Ovcharenko I, Loots GG, Giardine BM, Hou M, Ma J, Hardison RC, Stubbs L, Miller W (2005) Mulan: multiple-sequence local alignment and visualization for studying function and evolution. Genome Res 15:184–194. doi:10.1101/gr.300720

Paz-Ares J, Ghosal D, Wienand U, Peterson PA, Saedler H (1987) The regulatory c1 locus of Zea mays encodes a protein with homology to myb proto-oncogene products and with structural similarities to transcriptional activators. EMBO J 6:3553–3558

Pfaffl MW (2001) A new mathematical model for relative quantification in real-time RT-PCR. Nucleic Acids Res 1(29):e45. doi:10.1093/nar/29.9.e45

Pick TR, Andrea Bräutigam A, Schlüter U, Denton AK, Colmsee C, Scholz U, Fahnenstich H, Pieruschka R, Rascher U, Sonnewald U, Weber APM (2011) Systems analysis of a maize leaf developmental gradient redefines the current C_4 model and provides candidates for regulation. Plant Cell 23:1–13. doi:10.1105/tpc.111.090324

Sage RF, Zhu X-G (2011) Exploiting the engine of C(4) photosynthesis. J Exp Bot 62:2989–3000. doi:10.1093/jxb/err179

Saigo M, Bologna F, Maurino VG, Detarsio E, Andreo CS, Drincovich MF (2004) Maize recombinant non-C_4 NADP-malic enzyme: a novel dimeric malic enzyme with high specific activity. Plant Mol Biol 55:97–107. doi:10.1007/s11103-004-0472-z

Saigo M, Alvarez CE, Andreo CS, Drincovich MF (2013) Plastidial NADP-malic enzymes from grasses: unraveling the way to the C_4 specific isoforms. Plant Physiol Biochem 63:39–48. doi:10.1016/j.plaphy.2012.11.009

Sato Y, Takehisa H, Kamatsuki K, Minami H, Namiki N, Ikawa H, Ohyanagi H (2013) RiceXPro Version 3.0: expanding the informatics resource for rice transcriptome. Nucleic Acids Res 41:1206–1213. doi:10.1093/nar/

Schaaf J, Walter MH, Hess D (1995) Primary metabolism in plant defense (regulation of a bean malic enzyme gene promoter in transgenic tobacco by developmental and environmental cues). Plant Physiol 108:949–960. doi:10.1104/pp.108.3.949

Schmidt RJ, Ketudat M, Aukerman MJ, Hoschek G (1992) Opaque-2 is a transcriptional activator that recognizes a specific target site in 22-kD zein genes. Plant Cell 4:689–700

Schnable PS, Ware D, Fulton RS, Stein JC, Wei F, Pasternak S, Liang C, Zhang J, Fulton L et al (2009) The B73 maize genome: complexity, diversity, and dynamics. Science 326:1112–1115. doi:10.1126/science.1178534

Sell S, Hehl R (2004) Functional dissection of a small anaerobically induced bZIP transcription factor from tomato. Eur J Biochem 271:4534–4544. doi:10.1111/j.1432-1033.2004.04413.x

Sibéril Y, Doireau P, Gantet P (2001) Plant bZIP G-box binding factors. Modular structure and activation mechanisms. Eur J Biochem 268:5655–5666. doi:10.1046/j.0014-2956.2001.02552.x

Singh K, Dennis ES, Ellis JG, Llewellyn DJ, Tokuhisa JG, Wahleithner JA, Peacock WJ (1990) OCSBF-1, a maize ocs enhancer binding factor: isolation and expression during development. Plant Cell. doi:10.1105/tpc.2.9.891

Smith RG, Gauthier DA, Dennis DT, Turpin DH (1992) Malate and pyruvate-dependent fatty acid synthesis in leucoplasts from developing castor endosperm. Plant Physiol 98:1233–1238. doi:10.1104/pp.98.4.1233

Solano R, Nieto C, Paz-Ares J (1995) MYB.Ph3 transcription factor from *Petunia hybrida* induces similar DNA-bending/distortions on its two types of binding site. Plant J 8:673–682. doi:10.1046/j.1365-313X.1995.08050673.x

Tamura K, Peterson D, Peterson N, Stecher G, Nei M, Kumar S (2011) MEGA5: molecular evolutionary genetics analysis using maximum likelihood, evolutionary distance, and maximum parsimony methods. Mol Biol Evol 28:2731–2739. doi:10.1093/molbev/msr121

Van Doorsselaere J, Villarroel R, Van Montagu M, Inzé D (1991) Nucleotide sequence of a cDNA encoding malic enzyme from poplar. Plant Physiol 96:1385–1386

Veach YK, Martin RC, Mok DWS, Malbeck J, Vankova R, Mok MC (2003) O-glycosylation of cis-zeatin in maize. Characterization of genes, enzymes, and endogenous cytokinins. Plant Physiol 131:1374–1380. doi:10.1104/pp.017210

von Caemmerer S (2003) Furbank RT (2003) The C(4) pathway: an efficient CO(2) pump. Photosynth Res 77(2–3):191–207

Walter MH, Grima-Pettenatti J, Feuillet C (1994) Characterization of a bean (*Phaseolus vulgaris* L.) malic enzyme gene. Eur J Biochem 224:999–1009. doi:10.1111/j.1432-1033.1994.t01-1-00999.x

Wasserman WW, Sandelin A (2004) Applied bioinformatics for the identification of regulatory elements. Nat Rev Genet 5:276–287. doi:10.1038/nrg1315

Watson L, Dallwitz (1992) The grass genera of the world. C.A.B International, Wallingford

Wong AYM, Colasanti J (2007) Maize floral regulator protein INDETERMINATE1 is localized to developing leaves and is not altered by light or the sink/source transition. J Exp Bot 58: 403–414. doi:10.1093/jxb/erl206

Xue G-P, Bower NI, McIntyre CL, Riding GA, Kazan K, Shorter R (2006) TaNAC69 from the NAC superfamily of transcription factors is up-regulated by abiotic stresses in wheat and recognises two consensus DNA-binding sequences. Funct Plant Biol 33:43–57. doi:10.1071/FP05161